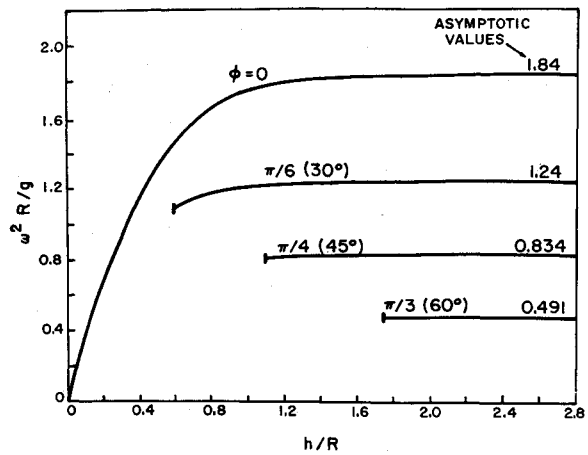

Fig. 2 Predicted variation of sloshing frequency with inclination angle and depth of fluid.

integrals in Eq. (4) are applied to give

$$J = \frac{1}{2}\rho\int_{t_1}^{t_2}\left\{\int_0^{2\pi}\int_0^R\int_{-h}^{\bar{z}}\nabla\varphi\cdot\nabla\varphi r dz dr d\theta - (g\cos\phi)^{-1}\int_0^R\int_0^{2\pi}[(\partial\varphi/\partial t)^2]_{z=\bar{z}}\, r d\theta dr\right\} dt \quad (5)$$

where $\bar{z}(r,\theta) = r\tan\phi\cos\theta$ is the distance from the plane $z = 0$ to the undisturbed free surface. It is also assumed, following Rattayya, that φ is expressible in the form

$$\varphi = \sum_{m=1}^{N}\alpha_m R^{-m}\psi_m(r,z)\cos\theta\sin\omega t \quad (6)$$

where α_m are constants, and each of the quantities $\psi_m\cos\theta$ is harmonic. The latter functions may be written as

$$\psi_m(r,z) = \sum_{k=0}^{m} a_k{}^m r^k z^{m-k} \quad (7)$$

where $a_k{}^m$ are constants determined by substituting Eq. (7) into the Laplace equation $\nabla^2(\psi_m\cos\theta) = 0$.

Substitution of Eqs. (6) and (7) into (5) gives, after integration over 1 cycle in time,

$$J = (\pi\rho R/2\omega)\left[\sum_{m=1}^{N} b_{mm}\alpha_m{}^2 + 2\sum_{m=1}^{N-1}\sum_{p=m+1}^{N} b_{mp}\alpha_m\alpha_p\right] \quad (8)$$

where

$$b_{mp} = b_{pm} = \sum_{k=1}^{m}\sum_{q=1}^{p} a_k{}^m a_q{}^p\left\{\frac{(\tan\phi)^{L+1}(kqI_{30}+I_{12})}{(L+1)(m+p+1)} - \frac{(-h/R)^{L+1}\pi(1+kq)}{(L+1)(k+q)} + \frac{(m-k)(p-q)}{L-1}\times\left[\frac{(\tan\phi)^{L-1}I_{10}}{m+p+1} - \frac{(-h/R)^{L-1}\pi}{2+k+q}\right] - \frac{F(\tan\phi)^L I_{20}}{(m+p+2)\cos\phi}\right\}$$

The parameters F, L, and I_{ij} are given in the Nomenclature. It is observed that the integral of Eq. (8) will be extremized when $\det[b_{mp}] = 0$.

For a specified number of terms (N) in the expansion for φ and given values of the angle ϕ and the geometric ratio h/R, it is seen that $\det[b_{mp}]$ is a function only of the dimensionless frequency parameter $F = \omega^2 R/g$. The numerical technique employed for determining F was as follows: Beginning with $N = 10$ and $F = 0$ the variation of $\det[b_{mp}]$ was developed until the determinant became zero. The value of N was increased by one and the procedure repeated. This iteration process was continued until successive values of F (for a zero determinant) differed by less than 1%. This degree of accuracy required values of N no larger than 12 for the cases considered. Because of the large order of the determinants involved it was necessary to employ double precision computation on an IBM 360 machine.

Some results of the foregoing computation program are illustrated in Fig. 2. These curves show the variation of $\omega^2 R/g$ with h/R for three nonzero inclination angles in addition to the exact solution[1] for $\phi = 0$ which was also obtained numerically as a check. Solutions were obtained only for those cases where the cylinder bottom was wetted, i.e., $h/R \geq \tan\phi$. Thus only for $\phi = 0$ does the frequency curve extend to the origin. It is also observed that the frequency decreases with increasing ϕ and that asymptotic values are reached in all cases for large h/R.

References

[1] Lamb, H., *Hydrodynamics*, 6th ed., Dover, New York, 1945.

[2] Abramson, H. N., ed., *The Dynamic Behavior of Liquids in Moving Containers*, NASA SP-106, 1966.

[3] Lawrence, H. R., Wang, C. J., and Reddy, R. B., "Variational Solution of Fuel Sloshing Modes," *Jet Propulsion*, Vol. 28, No. 11, Nov. 1958, pp. 729–736.

[4] Rattayya, J. V., "Sloshing of Liquids in Axisymmetric Ellipsoidal Tanks," AIAA Paper 65-114, New York, 1965.

Testing of Spacecraft Systems in a Simulated Ionospheric Plasma

D. R. Burrowbridge Jr.*
NASA Goddard Space Flight Center, Greenbelt, Md.

To test high-voltage systems adequately, one must consider the interaction between the charged particles of the ionosphere and the system's high electric fields. Failures and malfunctions in orbit have occurred that have been attributed to an interaction with the plasma.[1] The plasma effects on high-voltage systems include leakage currents, rf attenuation, large sheaths, inducement of outgassing, and possible catastrophic discharging.

Figure 1 shows the variation of charged-particle density vs height in the ionosphere.[2] Note the large day-night variation and the range of densities, 10^4–10^6 cm^{-3}. These charged particle densities produce an ion flux on the order of 10^{11} ions/sec-cm^2 as the result of the relative motion between the ions and spacecraft. Because of the high electron mobility, there is no directed electron flux.

The laboratory simulation is produced by creating a low-level discharge with an electron gun made of a nude ionization gage wired so that an electron beam is accelerated through the grid.[2] This beam produces ionization between two screens in the ion source, which is composed of four parallel screens. An electric field polarizes the plasma so that the ions are accelerated through the other screens into the test volume. The additional screens prevent high-energy-beam electrons from entering the test volume. This ion beam is neutralized by

Presented as Paper 70-169 at the AIAA 8th Aerospace Sciences Meeting, New York, January 19–21, 1970; submitted February 24, 1970; revision received March 30, 1970. The work of D. A. Huguenin in obtaining the electrolytic tank plots is gratefully acknowledged. The cooperation and assistance of the experimenters and NASA Goddard Space Flight Center personnel in the performance of these tests have been greatly appreciated.

* Aerospace Engineer.

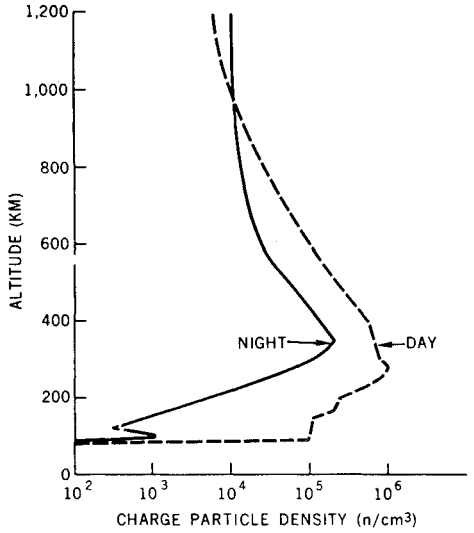

Fig. 1 Charged-particle density as a function of altitude.

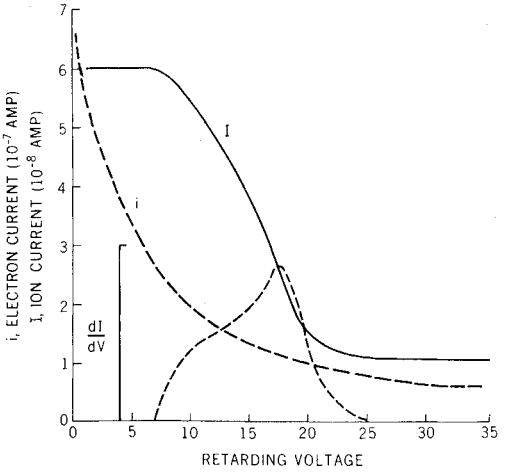

Fig. 3 Electron and ion currents as functions of retarding voltage.

electrons scattering and diffusing around the edges of the ion source. Figure 2 illustrates the electron gun.

Figure 3 shows typical energy profiles of the ions and electrons in the test volume. The ion energy can be varied from 2 to 40 ev with an energy spread (fwhm) of 1 to 6 ev. The electrons have a thermal velocity distribution corresponding to a temperature of 6 ev. Fluxes are measured with retarding potential analyzers.

The simulated ionosphere is characterized by an ion beam whose flux density duplicates that experienced in orbit. The electron density of the simulation is of the same order as that in orbit, but the electron temperature is about one order of magnitude larger.

These conditions are obtained in a vacuum chamber 4 ft in diam by 5 ft long. The ion beam is about 40 in. in diam. A mapping of the center of this beam shows a flux variation to 25% of max in a cylindrical volume 26 in. in diam by 20 in. long. The remaining volume still contains a plasma but the density and uniformity decrease near the walls. In larger vacuum facilities (7 ft × 8 ft and 12 ft × 15 ft) with the same source the beam uniformity and flux increase since wall losses are reduced. The electron energy is greater; it is about 20 ev, as opposed to 6 ev in the smaller chamber.

Ion species have not been duplicated: they are N_2^+ and N^+ in the laboratory simulation vs O^+, N^+, and H^+ in orbit. Neither has the pressure been duplicated: it is 10^{-5} torr, vs 10^{-8} torr or less.

Test Results

To date, tests have been performed for four different spacecraft programs: Orbiting Astronomical Observatory (OAO), Orbiting Solar Observatory (OSO), Applications Technology Satellite (ATS), and Orbiting Geophysical Observatory (OGO). The test item is typically an optical detector, high-voltage power supply, and current amplifier. The best test results are obtained when a test specimen in flight configuration is used so that actual effects can be determined, as opposed to testing with mock-ups and simulated detectors.

The plasma environment has been used to determine its effect on initiating or sustaining high-voltage breakdown and producing noise or false counts in open detectors. Potential shifts resulting from exposed potentials also have been observed.

One type of system that has shown itself to be particularly sensitive to the plasma is an optical system with an open-cathode photomultiplier. This detector, when exposed to a plasma, cannot distinguish between incoming photons and charged particles. In a plasma the detector is excited by ions as well as photons, and the output produced by ions can be sufficient to mask the measurement for which the experiment was intended. This type of experiment requires "ion traps" to exclude the plasma from the region of the detector.

Extensive studies were made on the ion trap design for the Goddard Experiment Package (GEP) for the OAO. Modification of the light baffle was examined as a means for effectively eliminating ions from the detector region. Figure 4 shows the modified light baffle used in the study. In the GEP, light enters the open end of the light baffle from a Cassegrain system that has an aperture of ≈38 in. The stops of the light baffle prevent scattered light from entering the detector region represented by the retarding potential analyzer. The modification consisted of adding ring electrodes to the stops. A study was made to determine the attenuation of the ion beam as related to the potential on the electrodes and their location. Figure 4 shows the equipotential lines produced by the most effective electrode configuration.[4] It produced the highest potential in the baffle and the greatest attenuation of the ion beam. The fraction of the total electric field between the electrodes as a function of position is represented by the equipotential lines, and indicates the potential gradient (trap potential) that a particle needs to overcome to pass through the ion trap. Particles with energies near or greater than the trap potential are generally only deflected, and in some instances actually focused, into an undesirable region.

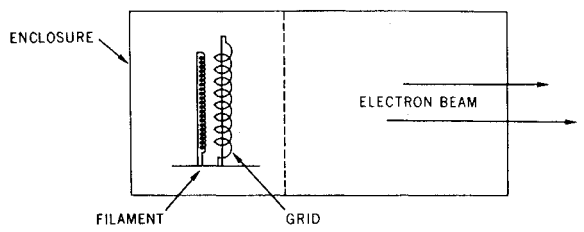

Fig. 2 Electron gun.

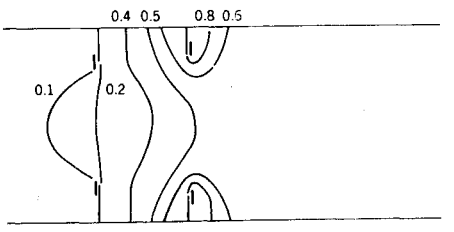

Fig. 4 Optimum ion trap.

In a plasma test with the modified light baffle the following results were obtained. The input current density corresponded approximately 6×10^{-7} amp/cm² ion current. The net ion flux was reduced 1000 times. The electron attenuation was a reduction from an electron current of 1×10^{-7} amp/cm² to $\frac{1}{30}$ of that value. This test determined the amount of attenuation that could be expected for the ion trap. However, the high-energy tail of the ion distribution and the high electron energy do introduce some uncertainty, but the test provides more information than the electrolytic plots as to the attenuation for marginal potentials.

The influence of the plasma on high-voltage breakdown was evidence in a test on the Harvard College Observatory OSO experiment. During this test, a plasma exposure at an elevated pressure of 10^{-3} torr and an ion flux of 5×10^{11} ions/cm²-sec, which corresponds to an orbital ion density of approximately 10^6 particles/cm³, produced arcing in the high-voltage system. These arcing conditions were not duplicated in a plasma-free environment until a pressure of 10^{-2} torr was reached. This would seem to indicate that the presence of the plasma produces an effective pressure that is higher than the actual pressure. It would not be unreasonable to assume that this effect is operative at lower pressures, in which case a plasma environment could induce breakdown when the pressure was "too low" to sustain it.

When a positive electrode is exposed in a plasma, it assumes the plasma potential and drives the other electrode negative with respect to the plasma. The amount of this potential shift is dependent on electrode voltages, areas, and the plasma parameters. The mechanism for this shift is the collection of plasma electrons by the positive surface. The collected electrons drive the other exposed surfaces negative until ions and electrons are collected in ratios that establish an equilibrium potential.

OGO-VI experienced such a potential shift. The potential of the spacecraft ground was driven about 26 v below the plasma potential. As a result, several experiments to measure plasma parameters did not have sufficient sweep voltages to determine the plasma parameters fully. The exposed positive potential is thought to have resulted from a short of the positive solar cell potential to the frame of the solar paddles. Exposed busses have produced similar potential shifts in other spacecraft. These potential shifts can also increase the energies of the ions or electrons that strike the spacecraft.

A test on a model of the OGO-VI power system in the simulated ionospheric plasma demonstrated that the potential shift could result from a shorted solar cell module, and displayed the proper functional behavior to duplicate the orbital observations.

Summary

This test environment has been extremely useful in demonstrating plasma-hardware interactions. These interactions can explain some malfunctions and failures observed in orbiting spacecraft. In light of these observations, tests should be made of high-voltage systems in a charged-particle environment so that their plasma susceptibility can be determined and, if necessary, corrected. The effectiveness of ion traps should be evaluated with consideration to higher-than-expected ion energies. The variable ion energy that can be obtained with this environment leads itself to the ion trap evaluation.

References

[1] Street, H. L. et al., "High Voltage Breakdown Problems in Scientific Satellites," X-300-66-41, Feb. 1966, NASA.

[2] Bourdeau, R. E., "Research Within the Ionosphere," *Science*, Vol. 148, No. 3670, April 30, 1965, pp. 585–594.

[3] Burrowbridge, D. R., "A Technique for Simulating the Ionospheric Plasma," *Proceedings of 14th Annual Institute of Environmental Sciences Technical Meeting*, Institute of Environmental Sciences, 1968, pp. 339–346.

[4] Einstein, P. A., "Factors Limiting the Accuracy of the Electrolytic Plotting Tanks," *British Journal of Applied Physics*, Vol. 2, Feb. 1951, pp. 49–55.

Prototype Electrolyzer for Oxygen Generation from Water Vapor

EZEKIEL L. SMITH* AND THEODORE WYDEVEN*
NASA Ames Research Center, Moffett Field, Calif.

Introduction

A WATER-VAPOR electrolysis cell[1–4] operates by passing a humid air stream continuously through one of the two compartments in the cell. Water vapor is then absorbed by the immobilized electrolyte H_2SO_4 in a silica gel matrix sandwiched between two platinum screen electrodes. A d.c. voltage sufficient for water electrolysis is imposed across the electrodes. The absorbed water is subsequently electrolyzed, generating oxygen at the anode and hydrogen at the cathode. The O_2 enters the air stream and the H_2 is collected. The H_2 and O_2 gases are prevented from mixing by a membrane that separates the two compartments. A recent theoretical study has shown that the water-vapor electrolysis unit should operate without impaired performance at reduced gravity.[5] This Note deals with a 104-day test of a $\frac{1}{4}$ man capacity ($\frac{1}{2}$ lb O_2/day) prototype unit for a space mission use.

Most experimental work with water-vapor electrolysis units has dealt with steady-state operation at a fixed set of experimental conditions. However, in a spacecraft cabin the unit probably would utilize the perspired and expired water vapor of the occupants and, therefore, would experience a range of both inlet humidities and temperatures. Therefore, the primary objective of this effort was to demonstrate the ability of the aforementioned unit to function reliably for a long time under varying atmospheric conditions of temperature and relative humidity within the acceptable range for human occupancy. A secondary objective was an

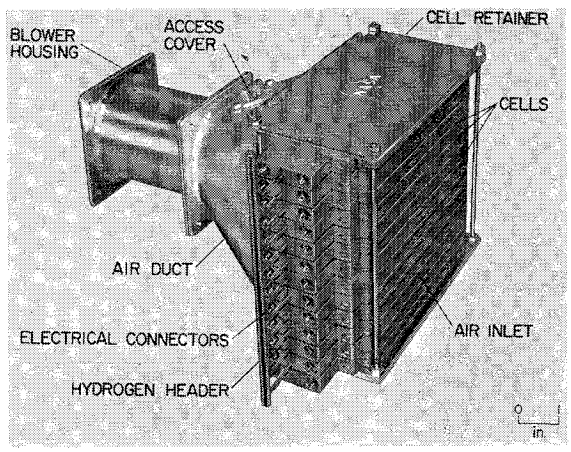

Fig. 1 One-quarter-man capacity water vapor electrolysis unit.

Received February 24, 1970; revision received April 17, 1970. Acknowledgment is made of the contribution of J. E. Clifford of Battelle Memorial Institute, Columbus, Ohio.

* Research Scientist.